THE UNIVERSITY OF OKLAHOMA

GRADUATE COLLEGE

COMPARISON OF THE MEASUREMENT CAPABILITIES OF CMM AND AA-CMM MACHINES IN FLATNESS VERIFICATION

A THESIS

SUBMITTED TO THE GRADUATE FACULTY

In partial fulfilment of the requirements for the

Degree of

MASTER OF SCIENCE

By

CESAR MARQUEZ RODRIGUEZ

Norman, Oklahoma

2022

COMPARISON OF THE MEASUREMENT CAPABILITIES OF CMM AND AA-CMM MACHINES IN FLATNESS VERIFICATION

A THESIS APPROVED FOR THE
SCHOOL OF INDUSTRIAL AND SYSTEMS ENGINEERING

BY THE COMMITTEE CONSISTING OF

Dr. Shivakumar Raman, Chair

Dr. Andres Gonzalez

Dr. Theodore Trafalis

Acknowledgments

I want to express my gratitude to all of those who have supported me professionally and personally all these years. I want to personally thank Dr. Raman for believing in me, providing me with an opportunity, and support to succeed during my master. I appreciate the trust you have invested on me, and I feel fortunate to have you as my mentor.

I would also like to thank my committee members for their help and support. I feel lucky to have experienced Dr. Gonzalez and Dr. Trafalis classes and being a witness to their passion for education and knowledge. To the administrators in the department who are always there to help us with pretty much whatever we need, thank you.

I would like to recognize Ricardo Palma for being there every time I need it help. Your guidance and support were tremendously helpful in the hard moments.

Finally, thanks to my family, Lucy, Alison, Ashly, Lorena, for whom I strive to be the best version of myself, and who will always support me no matter what. I love you all.

Table of Contents

List of Tables

List of Figures

Abstract

Manufacturing is among the most important activities contributing to the nation's economy. Almost everything we see, use, and touch, was made by someone, and now more than ever, quality is paramount across the industry. It is virtually impossible to fabricate perfect parts, and thus it is accepted to have variation in part dimensions specified by acceptable tolerances. For flatness, this tolerance will be the intended smallest variation of material form in a plane of a part. To control those variations and guarantee that the part will function as intended in an assembly, measurement verification must be conducted with specialized metrology equipment. The Coordinate Measuring Machine (CMM) and the Articulated Arm CMM (AA-CMM) are analyzed in this study, to identify their respective advantages and disadvantages in flatness measurement. Therefore, the goal of this pilot study is to identify the measuring limitations of each machine, to propose a methodology to identify appropriate use of each device based on its capabilities. Simple experiments were designed, and flatness measurements made. As expected, it is observed that the CMM performs better than the AA-CMM in flatness measurement. A more detailed statistical analysis must be made in the future to identify the quantitative differences in the use of these instruments, so that the versatility of AA-CMM in Geometry verification could be investigated.

Keywords: CMM, AA-CMM, Laser Point, Metrology device selection, Measurement boundary, Flatness verification

CHAPTER 1: INTRODUCTION

1.1 Introduction

Quality control has become a paramount process in most industries and successful organizations. In the manufacturing sector, "products develop certain external and internal characteristics that result, in part, from the type of production processes employed" (Kalpakjian & Schmid, 2014, p. 1030). Metrology science has defined those characteristics over the years and established methods and processes to inspect manufactured parts and guarantee that they meet specifications.

Usually, "external characteristics relate to dimensions, size, surface finish, and integrity; while internal characteristics include defects like porosity, impurities, inclusions, residual stresses, among others" (Kalpakjian & Schmid, 2014). These deviations are normal and expected, as it is virtually impossible to reproduce a part without variation. Therefore, in manufacturing, fabricated pieces are allowed to show characteristics that fall within a defined range known as tolerance.

The only way we can evaluate the parts, and consequently the performance of the process and the machines used, is by employing precision tools such as Coordinate Measuring Machines (CMM) and their more current counterpart, Articulated Arm Coordinate Measuring Machines (AA-CMM) also known as Coordinate Measuring Arm (CMA). Although these tools work under similar principles for obtaining data, they are utilized differently given that their physical structure and operation modes are unique. In the manufacturing sector, those differences have created a certain skepticism regarding the accuracy and reliability of the AA-CMM, which is often seen only as a reverse engineering tool.

A direct comparison of both machines, and the use of application methods on the shop floor of a company, could define the real-world limitations of each machine. This research presents some observations on metrology and quality control decision-making with regards to the use of AA-CMM.

1.2 Background

The fabrication of a part starts with the problem designers and engineers are trying to solve. At this point in the process, material requirements, stress analyses, rapid prototyping, fitment, and design for manufacturing (considering design feasibility under manufacturing constrains) of the part must all be performed. When the part is approved for fabrication, the bill of materials, process planning, and the drawing of the piece are completed. Drawings will often contain Geometric Dimensioning and Tolerancing (GD&T) in the form of a Feature Control Frame based on ANSI Y 14.5 M (1994).

GD&T is a crucial element of manufacturing parts within the expected quality standards. The "specified small amount that a part varies, also called *tolerance*, will not affect the part function, which makes it interchangeable" (Kalpakjian & Schmid, 2014, p. 1022). A part can be constrained on its *dimension* (height, width, depth, diameter, and angles) and its *geometry*, as shown in Table 1, courtesy of the American Society of Mechanical Engineers.

Table 1. Geometric Characteristics and its Symbols

GEOMETRIC CHARACTERISTICS SYMBOLS			
Feature	**Tolerance Type**	**Characteristics**	**Symbol**
Individual (no datum reference)	Form	Straightness	—
		Flatness	▱
		Circularity	○
		Cylindricity	⌭
Individual or Related	Profile	Of a line	⌒
		Of a surface	⌓
Related	Orientation	Angularity	∠
		Perpendicularity	⊥
		Parallelism	//
	Location	Position	⌖
		Concentricity	◎
	Runout	Circular runout	↗
		Total runout	⌰

Each of the tolerance types above describes different ways in which a piece can be characterized geometrically (overall *shape* of a feature or surface (GD&T Basics - Engineer Essentials, 2016)). For this investigation, we will focus on form tolerances, specifically *surface flatness*. This type of tolerance does not require a *datum reference* (theoretically exact axis, point, line, or plane (Kalpakjian & Schmid, 2014, p. 1024)), which could increase the chances of obtaining reliable data for comparison. The measures we use to compare the machines are independent of the precision level of the datum, and its interaction with the surface or fixture in which it is placed.

1.2.1 Surface Flatness

Groover (2010) defines flatness as "the extent to which all points on a surface lie in a single plane." In other words, "is the condition of a feature being purely in a 3D tolerance zone, given by the amount of variation on a vertical plane from the surface, over the entire 2D plane where the geometric tolerance is called. The tolerance zone for surface flatness is created by two parallel planes, separated by the part surface enveloped in between. Surface flatness is best measured by a CMM, and a change in angle would not affect it as long as the planes stay parallel. Moreover, when controlling the flatness of a surface, the straightness is also controlled in the two plane directions" (GD&T Basics - Engineer Essentials, 2016).

Geometric tolerance control, like surface flatness, is particularly important because the base of the part is usually flat and used as a datum reference to take other measurements (datum surface refinement). If the datum feature has deviations outside the tolerance, then the measurements on related features would be affected. Flatness can be measured on the machined, ground, and polished surfaces (Kalpakjian & Schmid, 2014, p. 1010).

Flatness calculation was time-consuming and required patience, as a height gage had to run across the surface, and the metrologist needed to check for needle amplitude. By utilizing a CMM and AA-CMM, the software can directly utilize the minimum zone method (calculate flatness error value) to evaluate flatness (FARO).

The minimum zone method "divides each data point into independent classes $C(xi, yi, zi)$ $(i = 1, 2, 3, \dots, n)$. The total number of classes is equal to the number of point cloud data in the sampling zone, and then the data points in the same plane are clustered on this basis. Then, the existing classes with three or more data points on the same parallel plane are clustered into new classes B (xj, yj, zj) $(j = 1, 2, 3, \dots, m)$, and the very high plane and the very low plane in the new class relative to the datum plane are the containment planes of the minimum zone method ($z = a_{max}x + b_{max}y + c_{max}$ & $z = a_{min}x + b_{min}y + c_{min}$). The points above and below the two planes are filtered according to the extremely high plane and the extremely low plane. The remaining points will be used as data points to evaluate the flatness error of the target" (Han, Chunlong, Jianyu, & Shenghuai, 2021).

The Best Fit method, "also known as RMS (Root Mean Square) plane, is an equation that will optimally fit a plane through your point cloud, finding an average while minimizing the effects of any outliers". For this method $RMS = \sqrt{\frac{h_1^2+h_2^2+h_3^2+\cdots+h_n^2}{n}}$. This calculations are also "sub-optimal when evaluating flatness, as the plane created by the algorithm is not necessarily parallel to the two virtual planes created to test for flatness. However, this method was used because it is robust, quick, and less calculation-heavy" (FARO). Because the CMM and its software only operate with the Best Fit method, that technique was chosen to test the data collected with the AA-CMM.

Previous studies show that CMMs are the most reliable method to test the flatness of a part. As we are trying to evaluate a real-world inspection scenario, we will be utilizing the software provided by the manufacturers of the machines employed in this research. The CMM and AA-CMM user interfaces are PC-DMIS and Geomagic Control X, respectively. Both software, can determine flatness form the measured plane of the part. Additionally, the system can graphically display if the piece is to specification by color coding with green, orange, and red when the value is below, close to, and above the established tolerance.

1.2.2 CMM and AA-CMM

Two metrology devices are being considered in this research. These devices are structured and operated differently. On their current setup, *contact* (probe to part touch) data can be obtained from the CMM and the AA-CMM, while *contactless* (not probe touch required) data can only be collected by the laser point in the CMA.

A "CMM consist of a platform on which the workpiece being measured is placed. A probe is attached to a head that can do various movements and records all measurements with contact on the part. They are very versatile and record measurements of complex profiles, with high resolution and speed" (Kalpakjian & Schmid, 2014, p. 1018). This machine requires a computer control, air lines to reduce friction on its movable parts, and some level of expertise to control the machine and operate the software (PC-DMIS). Unlike the AA-CMM, this device cannot be moved, can only be operated through software or a jog box control, and its measuring capabilities are limited to the volume the probe reaches.

AA-CMMs are "composed of rigid segments connected by rotary joints with 6 or 7 degrees of freedom, which are driven manually. High-resolution rotary encoders assist in the reading of each joint location. Subsequently, Cartesian coordinates of each measured point are calculated

according to the arm's kinematic model (Denavit–Hartenberg model) and the encoder readings. CMAs have portability and great flexibility, making them suitable for inspection tasks for assembly, in-process quality control, and in situ dimensional inspection or digitization for reverse engineering. Furthermore, the price of AACMMs is an incentive for workshop inspection processes where accuracy and repeatability requirements are lower, instead of acquiring expensive CMM equipment" (Cuesta , Gonzalez-Madruga, Alvarez, & Barreiro, 2014).

This device provides great flexibility as it can be moved to different places within a shop. The software is more intuitive, can work with a laptop, and provides data measured with a probe (contact) and a laser point (contactless). Unlike the CMM, this device cannot be used to take exactly the same coordinate data points in batch inspections, as is only manually operated, which in itself is cause of fatigue if used for extended periods of time. People within the industry believe that AA-CMMs should be mainly utilized for reverse engineering parts because it lacks the level of *resolution* and *precision* of the CMM.

Showed below is a matrix with relevant information regarding the machines and modalities mentioned earlier. These categories are relevant in the selection process of the machine. At an operational level, the machine shop must understand the cost of the machine, the space it takes, the maintenance, and the costs related to utilizing the machine. For example, CMMs after being coded for inspection, can be run part after part without much human input. However, when utilizing the AA-CMM in both modalities, an operator must control the machine at all times for all the parts being inspected. Meaning that if a part is being mass produced, the shop will be hiring an operator that can solely work on the AA-CMM, which depending on the scenario, could be a potential source of waste on the process and on the budget (AAA Testers; Metrology Deals; FARO).

Table 2. Technical machine information from vendors and suppliers

Machine Information	CMM	FARO TIP	FARO LP
Cost (USD)	26,500	18,000	FARO TIP+2,000=20,000
Measuring Range (inches)	19x19x14	44	44
Footprint (ft)	4x4x8	1x1x2	1x1x2
Operation Mode	Manual/Automatic	Manual	Manual
Axis	3-axis	6-axis	7-axis
Vector Method	Orthogonal	Denavit-Hartenberg	Denavit-Hartenberg
Data Collection	Contact	Contact	Contactless
Single Point (inches)	0.0002	0.001	0.0012
Volumetric Accuracy	0.0004	0.0014	0.0017
Operating System	PC-DMIS	Geomagic Control X	Geomagic Control X
System Requirement	CPU & Compressed Air	NA	NA
Calibration (years)	5	1	1
Calibration Cost (USD)	NV	2,000	550
Standards	NV	ISO 17025	ISO 17025
Battery	NO	YES	YES
Temperature and Overload Sensors	NO	YES	YES

1.2.3 Terminology

Here we present, in alphabetical order, other commonly used terms that help define geometric characteristics and their measurements, which are detailed in greater depth in the ANSI/ASME B4.2, ANSI/ASME Y14.5, and ISO/TC10/SC5 (Kalpakjian & Schmid, 2014, p. 1024) and (Groover, 2010, p. 79).

- Accuracy: Degree to which the measured value agrees with the true value of the quantity of interest
- Allowance: The specified difference in dimensions between mating parts.
- Dimension: Numerical value expressed in appropriate units of measure and indicated on a drawing and in other documents along with lines, symbols, and notes to define the size or geometric characteristics of a part or feature.
- Measurement: When an unknown quantity is compared with a known standard.
- Precision: Sometimes incorrectly called accuracy, it is the degree to which the instruments give repeated measurements of the same standard.
- Resolution: The smallest difference in dimensions that the measuring instrument can detect or distinguish.

CHAPTER 2: BACKGROUND

2.1 Summary

"Each of the 6 million parts of a Boeing 747-400 aircraft requires measuring about 25 features, representing a total of 150 million measurements" (Kalpakjian & Schmid, 2014, p. 1022). All of those measurements will be done with highly specialized equipment among which the CMM will be the most popular. It is essential to understand potential alternatives to completing metrology work in this scenario, or even in a smaller manufacturing shop. It all will depend on the required tolerances, and the limitations of machines such as CMMs and AA-CMMs. In this chapter we will delve into an understanding of the importance of metrology, the differences between the aforementioned devices, previous research on the topic, and how we will be approaching the sample data for our experiment.

2.2 Literature Review

"In addition to mechanical and physical properties of materials, other factors that determine the performance of a manufactured product include the dimensions and surfaces of its components" (Groover, 2010, p. 78). As we discussed earlier, is virtually impossible or just too expensive to produce parts that are exact replicas of each other. Parts are given allowances that permit components to fit together during assembly. Still, in order to control those allowances the manufacturer must inspect the part and make sure it was produced within the tolerance specifications dictated on the design.

Tolerances exist in three forms. Bilateral tolerance where the variation is permitted in both positive and negative directions from the nominal size. Unilateral, where the variation is permitted in one direction. Limit dimensions are an alternative method where the maximum and minimum dimensions allowed are given without a nominal size (Groover, 2010, p. 79). Most

tolerances highly depend on the type of manufacturing process the part undergoes. For example, a machined part creates significantly smaller tolerances than casting. Milling's typical tolerance is $\pm 0.003\ in$, for Turning is $\pm 0.002\ in$, and all of these tolerances increase with part size, as shown in Figure 1 in the appendix (Groover, 2010, p. 94).

In order to manufacture a part, cutting conditions, also known as machining parameters, "are selected based on rules of thumb, handbooks, or other published guides. The Machinability Data Handbook provides a starting set of cutting conditions which are usually conservative and apply only to a particular machining situation" (Stephenson & Agapiou, 1997, p. 796). By knowing the type of material and process employed during manufacturing, machinists obtain initial values for spindle speed, feed rate, and depth of cut. These machining parameters are specifically utilized to maintain material integrity, prolong tool life, and obtain a quality surface finish, which is paramount result of the machining process. A good surface finish will get the part into the appropriate tolerances. "The recommended conditions are reviewed based on the tolerances needed. In today's economically competitive environments, focusing on high quality, it is quite likely that tight tolerances and very good surface finish are being specified" (Trent & Wright, 2000, p. 399). Kalpakjian and Schmid also mentioned that surveys showed dimensional tolerances on state-of-the-art manufactured parts are shrinking by a factor of 3 every ten years, and that this trend will continue.

The demand for tighter tolerances and improved quality, shows that engineering metrology continues to be applied and must continue to be studied, to provide tools or techniques that improve the resolution and precision of the measurements. "Traditionally, measurements have been made after the part has been produced (post-process inspection). Today, measurements are being made while the part is produced on the machine (in-process, online, or real-time

inspection)" (Kalpakjian & Schmid, 2014, p. 1008). That way, machining parameters can be adjusted to compensate for any changes in the tool, coolant, and temperature. Thus, reducing waste and increasing productivity, as usually, qualitative metrics like chip color (silver=low speeds, blue=high speeds) or surface touch are utilized by machinists to determine what is happening during the manufacturing process (Trent & Wright, 2000, p. 398).

Different tools have been developed over the years for metrology purposes. Among the best, we have the CMM machine. The ability to code in inspection points, and complete analysis within its software, allows it to be utilized several times for the same inspection process without much input or interaction from an operator. There are several studies done on CMM machines, their calibration, and precision. However, their limited flexibility and workspace make modern AA-CMM machines great candidates to conduct measurements. Nevertheless, in most of the research work cited in this paper, the general consensus was that CMMs performed better that AA-CMMs; which is the general belief of shop quality workers, and why these machines are preferred for reverse engineering. The error and lack of repeatability encountered in AA-CMMs are believed to come from the way in which they utilize angles to locate point coordinates, while CMMs operate with orthogonal values.

Lu, et al. (2013) modeled and analyzed the error of AA-CMMs by looking into the Denavit-Hartenberg (D-H) method, which is the kinematic model utilized by CMAs, as shown in Figure 2 in the appendix. They created an error model that functions as theoretical foundation for calibration and compensation. Similarly, Acero et al. (2016) utilized the D-H method to calculate virtual distances after the AA-CMM was attached to an Index Metrology Platform, to create an alternative verification technique that evaluated the volumetric performance of the AA-CMM.

These papers focus on figuring out methodologies to calibrate CMAs and improve their reliability in the field.

Cuesta, et al. (2014) went even further by creating a concept for a feature-based gauge and utilized it to assess AA-CMM performance and reliability for the evaluation of geometric tolerances. They too, utilized the process to quantify the uncertainty in the calibration process, and "included the operator contribution to the measurement results as an inherent part of CMA performance." To evaluate the data, they compared the measurements taken with the AA-CMM against the ones given by the CMM, resulting in the "proposed gauge being a suitable instrument for AA-CMM evaluation. And, for tests as defined per AA-CMM international standards, including the ability to qualify operator skill to reduce operator's negative impact. A large part of CMAs measurement variability is assigned to the operators-influence, since they control many of the measurement parameters. According to the morphology of each feature, operators may adapt their measuring technique with influence on important factors such a point distribution, slipping tendency, contact force or accessibility." The repeatability issues mentioned earlier can be controlled by minimizing the operators influence, and with proper measurement techniques like point distribution (Cuesta, Alvarez, Barreiro, & Gonzalez-Madruga, 2014).

Regarding direct comparisons utilizing the mentioned metrology devices, as intended from the factory, we could not find any specific research. There is not an establish methodology or guide for manufacturing shops to understand the limitations of the CMMs and AA-CMMs in this conditions. Therefore, it is crucial to test the working range of these machines without incorporating particular calibration methods and gauges. Even though the cited research allows us to understand the shortcomings of the AA-CMM, it will be really imperative to show the

measurement capabilities of the machine, particularly when testing contact and contactless scenarios and provide numerical boundaries for the usage of these machines.

2.2.1 Sampling Methods

To compare the machines, we must be able to collect robust data. One of the main constrains regarding this research, is the way in which we can obtain the coordinate points from each machine. The CMM can repeat given points several times with accuracy, as it is computer controlled. The AA-CMM is manipulated by an operator that will quite likely not hit coordinate points accurately part after part. As we are comparing contact and contactless data points, we must focus on how to properly sample data in both modalities. Lopez (2019), tested flatness on a CMM by utilizing sampling methods like Align Systematic, Halton-Zaremba, and Hammersley; then compared the results to a laser point scan on an AA-CMM. This does not represent a direct comparison of the sample data for our purposes. Besides, it requires precise positioning of the probe in the part, which as we previously mentioned, is difficult to do when manually operating the probe. Therefore, when collecting contact data for our experiment, it was deemed appropriate to employ Simple Random Sampling.

"This technique is achieved by collecting n sample points from a population of N points where each point has an equal chance of being selected. For this reason, we select a set of random coordinates within the specified range for $x\ and\ y$ (which depends on the alignment and dimensions of the part) for each part." (Gupta, 2017). By utilizing this method, we are free to select random points from the surface of the piece, as long as orientation and alignment are kept equal. In the case of the CMM, the points are picked randomly through the controller, saved, and then reproduced on the following parts automatically, while for the AA-CMM, the points are just

picked randomly every time. This makes sense, as CMMs are meant to be used with a specific program that inspects the same coordinate points part after part.

Regarding the number of points to be collected in the sample, Gupta, quoted Kim et al. (2000), who established that a sample size beyond the size of 64 shows the most accurate inspection results while measuring flatness of a surface. Gupta collected three different sample sizes to show the effect of sample types and sizes on the inspection. Then she concluded that "parallelism was best measured with larger sample sizes that have been selected randomly, as aligned sampling might have systematic errors which might go undetected with larger samples" (Gupta, 2017).

For the contactless format, the amount of data collected cannot be controlled as well as can be with the probe. The amount of data will depend on the number of passes the laser line does on the part. Other measurement controls are proposed by Vijayarangan (2017), such as performing the scans in a controlled environment free from direct sunlight to avoid luminosity on the scanning area and using a dull spray to avoid reflectivity of the laser on the part.

2.3 Problem Definition

As shown, much of the research on AA-CMMs relates to creating accurate calibration systems and methodologies to reduce errors when inspecting a part. Regarding the direct comparison of CMMs and CMAs, the studies focus on error validation and the poor repeatability of measurements on the CMA. There is a knowledge gap worth studying when it comes to comparing both of these metrology machines. It is clear that AA-CMMs do not perform as well as CMMs specifically in product verification, but there is not much relevant information regarding the limitations of their measurement capabilities and their significance in a shop floor. Both devices operate differently and are almost opposites regarding advantages and

disadvantages, which can be of value to certain manufacturers, as they also operate differently on the type of work they provide, their capabilities, the project itself, and the operational budget of that company.

Therefore, the importance of this research is not just to show that these machines are different. But to understand how they differ on their measured outputs and create boundaries that will allow machine shops to recognize the limitations of the equipment, as some shops might not require the resolution and precision that a CMM offers.

This research aims to define the differences between CMM and AA-CMM for the particular devices in the experiment, as they are often likely to be used in the factory by utilizing contact and contactless measured data to obtain flatness values. Those values will define machine use boundaries. These will help machine shops with metrology device purchasing, proper device usage, accepting or rejecting bids, or guarantying quality assurance at different levels of a project.

In the following chapter, we will discuss the methodology for the experiment in this research, and in chapter 4 we will proceed to look at the results, analyze the data, and ultimately draw conclusions.

CHAPTER 3: METHODOLOGY AND EXPERIMENTATION

3.1 Methodology

3.1.1 Apparatus

The data collection is divided into two parts, contact and contactless sampling, and requires two types of machines: CMM and AA-CMM. For contact data collection, we utilized two machines. The Brown & Sharpe®, MicroVal™ PFx 454 CMM, which utilizes PC-DMIS as the user interface and computer control, and a Renishaw® tip with Ruby ball/stainless steel stem A-5000-3554 as the probe that touches the part. For the AA-CMM, we employed a Faro Arm® Platinum, which utilizes Geomagic® Control X™ as the user interface, and a zirconia ball A-5003-7673 with $0.11811 in$ diameter as the probe that touches the part.

For contactless sampling, the Faro Arm® Platinum is equipped with a V3 Laser Line Probe. This setup works with the same software as the contact AA-CMM data sampling.

Microsoft Excel is another necessary software to store the data in a combined format for analysis, and RStudio is utilized to complete data analytics.

Six fixtures are needed to secure the samples in place while collecting the data. Three are to be positioned in the metal workbench of the AA-CMM, and the other three are on the granite table of the CMM. They must be placed so that parts can be changed with ease and secured in place.

3.1.2 Samples

This study utilizes 15 aluminum blocks of $2.5 \times 2.5 \times 0.5\ in$, with a tolerance of $\pm 0.01\ in$. Five replicates are not machined. We considered those to have a 0° top angle. Ten of the blocks have been machined with an angle on the $2.5 \times 2.5\ in$ surface. Five replicates have a top angle of 5°, and five have a top angle of 10°, as shown in Figure 3. The samples were

measured in an environment of approximately 68°F. An alignment is completed for each part separately. For the angled tops, the origin point was on the left corner of the shortest height, as shown in Figure 4. Flat tops origin was on a left corner of any possible vertex. Orientations were assigned on the software of both machines, and marked on the aluminum, to keep the same alignments for repeatability of the experiment.

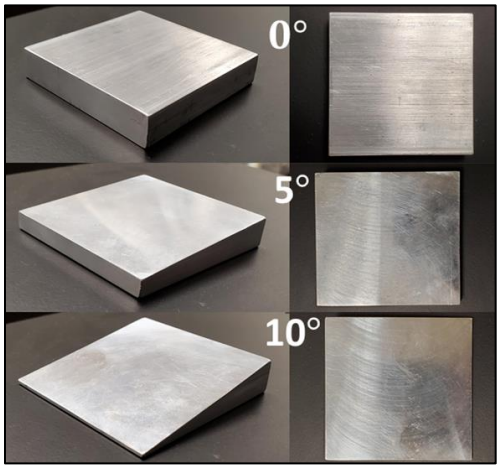

Figure 3. Sample types

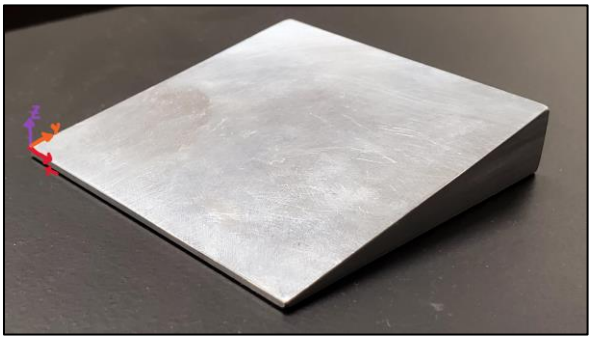

Figure 4. Machined sample part showing the alignment introduced in the software

3.1.3 Contact Data Collection

As discussed in Chapter 2, to have a robust data set in random sampling, we must collect at least 64 data points. For the purposes of this research, we rounded that value up to 70 data points to be collected on the CMM and the AA-CMM. Even though the data is being collected randomly, we applied two rules to control the error created by the operator of the AA-CMM. First, only one person is responsible for collecting all the data in both machines and modalities. Second, as valleys and peaks can form from the pressure the fixture or the vice insert on the part when it is being machined, we made sure to collect data points in the corners, edges, and the surrounding area to the center of the parts in both metrology devices, as shown in Figure 5 and 6.

Figure 5. PC-DMIS virtual representation of the probe and the points on the surface of the part

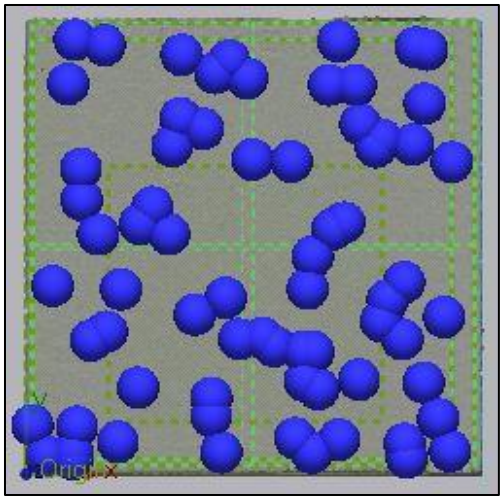

Figure 6. Geomagic virtual representation of the points on the surface of the part

Figures 7 and 8 show a flow process diagram for the CMM and AA-CMM contact data collection, with all the steps followed to obtain the necessary data.

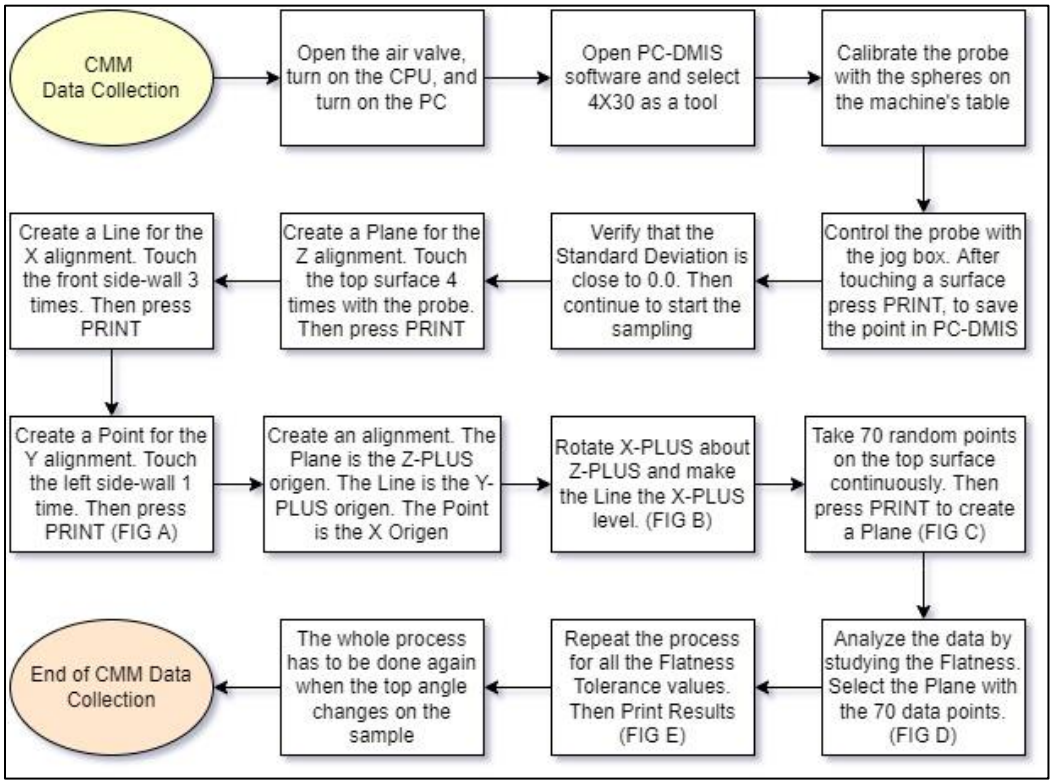

Figure 7. Flow process diagram of CMM contact data collection. FIG A-E are on the appendix.

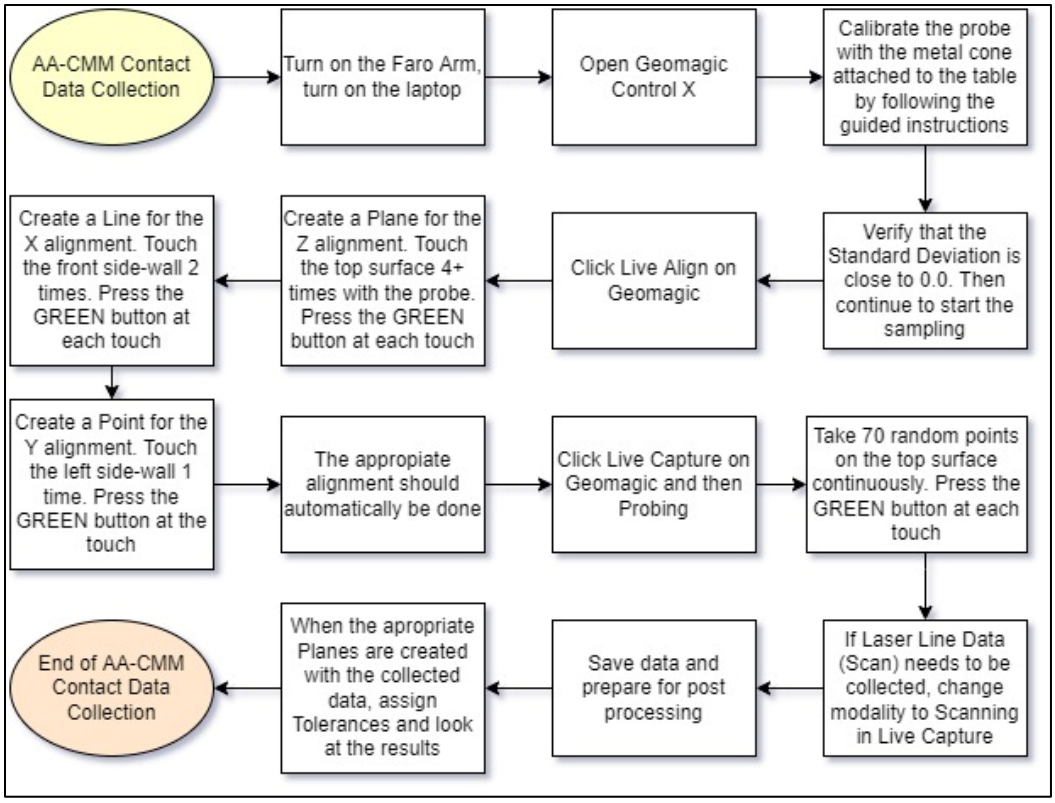

Figure 8. Flow process diagram of AA-CMM contact data collection

The data from the software results on flatness, was typed into an excel sheet, where it can be easily compared, organized, and used to create visual aids.

3.1.4 Contactless Data Collection

In order to collect this data, the lights were turned off, leaving the room dark enough to see the laser of the scanner reflect on the table and the part. The positioning of the laser with respect to the part was practiced, guaranteeing quality data. At least six passes of the laser were completed per part. The steps shown in Figure 9 explain how the contactless data was collected.

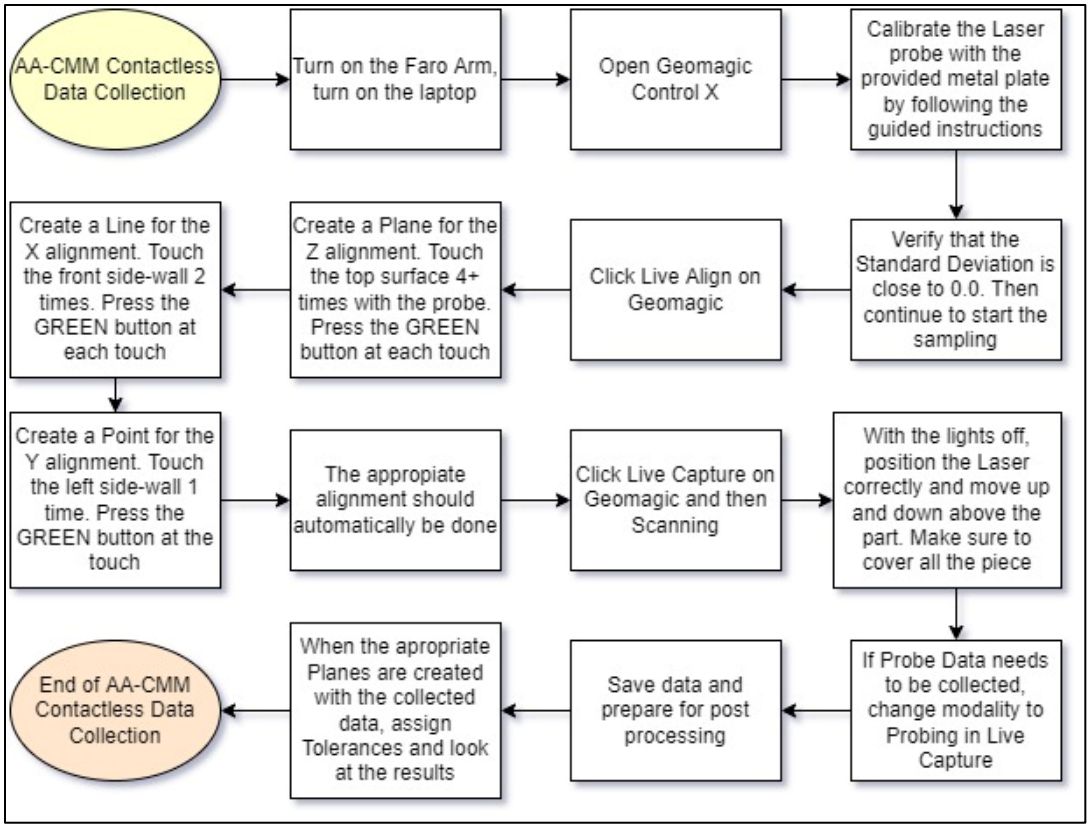

Figure 9. Flow process diagram of AA-CMM contactless data collection

The data from the software results on flatness, was also typed into an excel sheet, where it can be easily compared, organized, and used to create visual charts.

This experiment was repeated under the same conditions two more times. The replicates of the experiments are expected to make the data more robust, test the repeatability of the test, and help us understand the precision and accuracy of the gauges.

3.2 Data Post-Processing

Each data sample was compared to different tolerance levels for flatness, which are smaller than the tolerance dimension of $\pm 0.01\ in$ for which the part was designed and controlled. Meaning that at that tolerance level, the part should pass the inspection regardless of the modality and machine where the data was collected. These tighter tolerances were chosen based

on practical experience and what is common to see on the manufacturing floor. The other tolerance values applied to flatness were $0.005in, 0.003in, 0.002in, 0.001in, and\ 0.0001in$.

As mentioned in the process flow diagrams for the AA-CMMs in both contact and contactless modalities, after the data is collected, it must be post-process to obtain planes that the system can utilize to check the tolerances. For Geomagic® Control X™, the point data of the probe sampling is highlighted and then a geometric feature, in this case a plane, is selected from the menu. This created a plane that was used to obtain the flatness value of that particular part. The process was then repeated in all the parts. Another important post-processing step is to curate the data obtained with the laser point. Given that in some scenarios, the data comes with outlier points, data from the sidewalls of the part, or data points from the fixtures that are holding the part which get pick up by the laser, as shown in Figure 10.

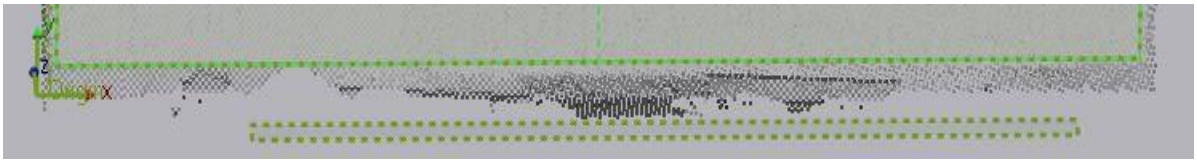

Figure 10. Scanned data points include some data from sidewalls of the piece. Keeping this data would alter the results

Moreover, as shown in Figure 11, data picked up by the laser might not be evenly distributed, as this highly depends on the number of passes and the scanner position with respect to the part.

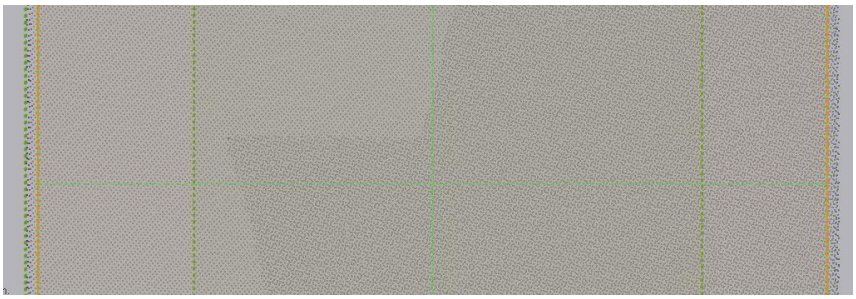

Figure 11. Scanned data points show that data collected is denser in certain parts of the piece for some of the samples

Therefore, when selecting the plane to create the tolerance evaluation, we selected a square of data towards the center of the piece, leaving some margin on the sides, to avoid picking unwanted data, as shown in Figure 12.

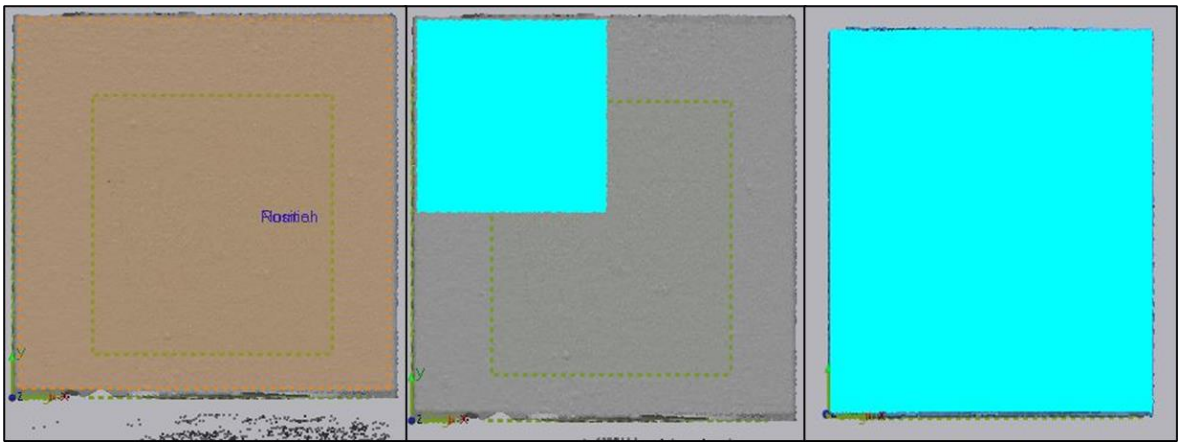

Figure 12. Point data including outliers and noise, are cut out by selecting an inner plane that has better quality data

CHAPTER 4: DATA ANALYSIS AND DISCUSSION

4.1 Results

Flatness data was utilized to create data plots that help us to better understand the experiment results. The data presented below shows all the samples of the three different tests in the x-axis, and their respective flatness values in the y-axis, grouped by machine type and part degree cut. The red lines represent, what we called “the working envelope.” These are the areas where the dependent variable exists and changes depending on the sample. The data points outside this envelope are considered outliers in our visual analysis, as they do not follow an acceptable pattern and deviate significantly from the behavior shown by their other test’s counterparts.

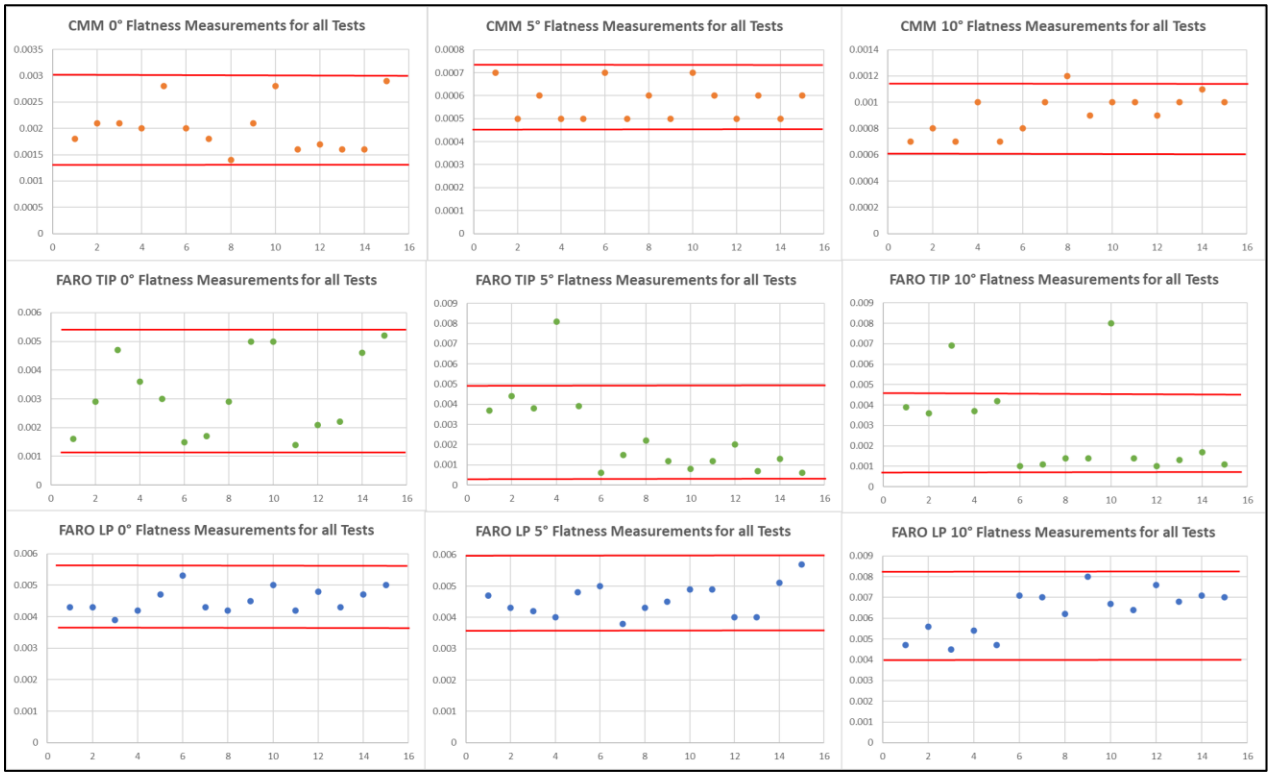

Figure 13. CMM, AA-CMM contact and contactless measured flatness plotted for each tested sample (replicates included)

To visually assess the boundaries of each machine based on the given tolerances, the following Tables 3, 4, and 5 were created. The color coding is directly obtained from the

software of both machines, which graphically tells the operator which parts are within (green), close to (orange), or out (red) of specifications.

Table 2. Color-coded flatness evaluation for test 1 CMM measured data based on different tolerance levels

CMM Measured Flatness	Part	Tolerance					
		0.01	0.005	0.003	0.002	0.001	0.0001
	Part1D0						
	Part2D0						
	Part3D0						
	Part4D0						
	Part5D0						
	Part1D5						
	Part2D5						
	Part3D5						
	Part4D5						
	Part5D5						
	Part1D10						
	Part2D10						
	Part3D10						
	Part4D10						
	Part5D10						

Table 3. Color-coded flatness evaluation for test 1 AA-CMM contact measured data based on different tolerance levels

AA-CMM Laser Point Measured Flatness	Part	Tolerance						Data Points
		0.01	0.005	0.003	0.002	0.001	0.0001	
	Part1D0							36410
	Part2D0							22164
	Part3D0							38760
	Part4D0							39994
	Part5D0							32771
	Part1D5							42189
	Part2D5							44129
	Part3D5							36778
	Part4D5							40261
	Part5D5							39477
	Part1D10							11846
	Part2D10							38871
	Part3D10							11272
	Part4D10							31479
	Part5D10							32058

Table 4. Color-coded flatness evaluation for test 1 AA-CMM contactless measured data based on different tolerance levels

AA-CMM Tip Measured Flatness	Part	Tolerance						Number of Points
		0.01	0.005	0.003	0.002	0.001	0.0001	
	Part1D0							70
	Part2D0							70
	Part3D0							70
	Part4D0							70
	Part5D0							70
	Part1D5							70
	Part2D5							69
	Part3D5							70
	Part4D5							69
	Part5D5							70
	Part1D10							68
	Part2D10							69
	Part3D10							70
	Part4D10							70
	Part5D10							70

We obtained a box plot chart, that helps us shine some light on the potential distribution of the data, as shown in Figure 14.

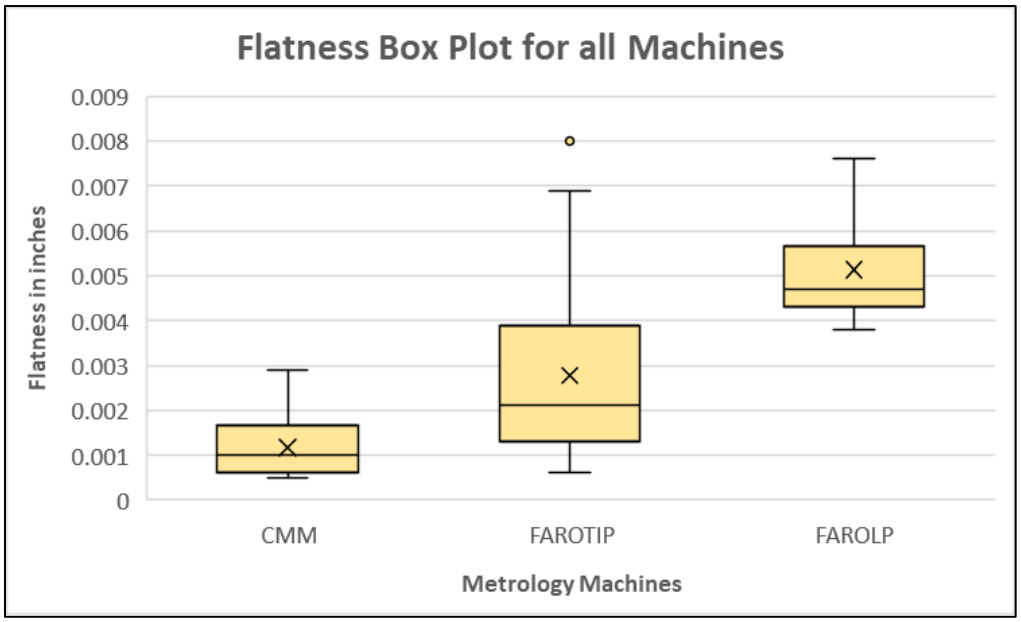

Figure 14. Box plot for flatness by metrology machines

Three tables were created. Table 5 contains the average flatness of all same angled parts per their respective machines. Table 6 and 7, contain the maximum and minimum flatness recorded per their respective machine and angle.

Table 5. Average part flatness for all tests based on machine and degree combination

MEAN	D0	D5	D10
CMM	0.0020	0.0006	0.0009
FAROLP	0.0045	0.0045	0.0063
FAROTIP	0.0032	0.0024	0.0028

Table 6. Maximum recorded flatness for all tests based on machine and degree combination

MAX	D0	D5	D10
CMM	0.0029	0.0007	0.0012
FAROLP	0.0053	0.0057	0.008
FAROTIP	0.0052	0.0081	0.008

Table 7. Minimum recorded flatness for all tests based on machine and degree combination

MIN	D0	D5	D10
CMM	0.0014	0.0005	0.0007
FAROLP	0.0039	0.0038	0.0045
FAROTIP	0.0014	0.0006	0.001

Finally, in order to validate the findings of the experiment, a gauge and measurement system capability study was done with the data points collected. Different gauge capabilities studies were utilized, as the implementation of these methods vary widely across the industry. The study thresholds selected for this research, are commonly used for the different techniques. However, these thresholds can change depending on the requirements of the project (Montgomery, 2013, pp. 379-387).

In order to calculate most of the gauge capacity equations, the gauge variance (σ^2_{gauge}) must be found. Given that:

$$\sigma^2_{gauge} = \sigma^2_{Repeatability} + \sigma^2_{Reproducibility} = \sigma^2 + \sigma^2_O + \sigma^2_{OP}$$

$$\sigma^2 = MS_E \qquad O = Operator \qquad P = Part$$

Because only one operator completed all the data collection of the within-subject design experiment with replicates, the reproducibility of the experiment is not being considered, just the repeatability. Therefore:

$$\sigma^2_{gauge} = \sigma^2_{Repeatability} = \sigma^2 = MS_E$$

Consequently, the following equations were applied, and the results collected. Remember that all of these measurements are arbitrary and depend on the application, and the engineers responsible of determining what the threshold of the machine should be for a particular inspection process.

- Precision-to-Tolerance (P/T) ratio: If P/T ≤ 0.1 adequate gauge capability can be implied

$$P/T = \frac{k\hat{\sigma}_{Gauge}}{USL - LSL}$$

	P/T	0.01	0.005	0.003	0.002	0.001	0.0001
CMM	D0	0.0001464	0.0002928	0.000488	0.000732	0.001464	0.01464
	D5	0.0000042	0.0000084	0.000014	0.000021	0.000042	0.00042
	D10	0.0000088	0.0000176	2.93E-05	0.000044	0.000088	0.00088
FAROLP	D0	0.000084	0.000168	0.00028	0.00042	0.00084	0.0084
	D5	0.0001786	0.0003572	0.000595	0.000893	0.001786	0.01786
	D10	0.0001728	0.0003456	0.000576	0.000864	0.001728	0.01728
FAROTIP	D0	0.001408	0.002816	0.004693	0.00704	0.01408	0.1408
	D5	0.0008456	0.0016912	0.002819	0.004228	0.008456	0.08456
	D10	0.00224	0.00448	0.007467	0.0112	0.0224	0.224

- Measurement System Variability: Fraction of the total observed variance attributed to the machine

$$\rho_M = \frac{\sigma^2_{Gauge}}{\sigma^2_{Total}} = 1 - \rho_P$$

ρM	D0	D5	D10
CMM	0.127548	0.148936	0.385965
FAROLP	0.203488	0.154793	0.166186
FAROTIP	0.155645	0.299858	0.37623

- Processed Part Variability: Fraction of the total observed variance attributed to the part

$$\rho_P = 1 - \rho_M$$

ρP	D0	D5	D10
CMM	0.872452	0.851064	0.614035
FAROLP	0.796512	0.845207	0.833814
FAROTIP	0.844355	0.700142	0.62377

- Signal to Noise Ratio: If SNR ≥ 5 adequate gauge capability can be implied. An SNR ≤ 2 indicates inadequate capability

$$SNR = \sqrt{\frac{2\rho_P}{1-\rho_P}}$$

SNR	D0	D5	D10
CMM	3.698693	3.380617	1.783765
FAROLP	2.797958	3.304617	3.167763
FAROTIP	3.293891	2.160977	1.820959

- Discrimination Ratio: If DR ≥ 4 adequate gauge capability can be implied

$$DR = \frac{1+\rho_P}{1-\rho_P}$$

DR	D0	D5	D10
CMM	14.68033	12.42857	4.181818
FAROLP	8.828571	11.92049	11.03472
FAROTIP	11.84972	5.66982	4.315893

4.2 Data Analysis

As expected, the studied CMM machine has a better resolution than both modalities in the AA-CMM machine. As it can be seen in Figure 13, the CMM measured flatness for 0° samples ranges from measurements close to $0.001\ in$ to no more than $0.003\ in$, while the AA-CMM contact and contactless recorded values range from almost $0.001\ in$ to about $0.006\ in$, and from just below $0.004\ in$ to $0.006\ in$ respectively. These higher flatness values were expected, as the part without the surface cut (0°) had a rougher surface finish than the part with the angled cuts. However, when we contrast the measured flatness for the parts with the machined surface (5°,10°), it can be seen that the CMM highest recorded value is below $0.001\ in$ for the 5° part, while for the AA-CMM contact modality, $0.001\ in$ is just about the minimum value recorded. Similar observations can be made when comparing the other provided tables for different degree/machine combinations.

The number of points that the laser can capture does not appear to have an effect on the flatness value measured, because even though the number of points widely vary in each scan, the recorded data for different replicates does not appear to be changing drastically as seen in Figures 13 and 14 for FAROLP.

Figure 14 shows that the CMM data, while positively skewed, registered the majority of flatness measurements to be just around $0.001in$ ($0.0012in$). While the AA-CMM with a probe is similarly on the positive skewed side and has a mean of just above $0.002\ in$ ($0.0028in$), and it contains the most outliers. In the case of the laser scan, the mean is just above 0.005in ($0.0051in$) and still positively skewed. Consequently, the contact modality in the CMA appears to perform slightly better than its contactless counterpart, but still not as good as the as the CMM data, assuming that a good performance will be given by the machine which can measure small flatness readings.

To guarantee that there are significant differences between the CMM and AA-CMM modalities, we conducted a within-subject design ANOVA utilizing RStudio (code and results in the appendix). This investigation does not consider the effect of the operator, as only one individual performed the experiment. Therefore, our model is as follows:

$$H_0 = \tau_{\alpha 1\beta 1} = \tau_{\alpha 2\beta 2} = \cdots = \tau_{\alpha 3\beta 5} \qquad H_1 = not\ H_0$$

$$Y_{ijkl} = \mu + \alpha_i + \beta_j + \gamma_k + (\alpha\beta)_{ij} + \varepsilon_{ijkl}$$

$$Where$$

$$i = CMM, FAROTIP, FAROLP$$

$$j = 0°, 5°, 10°$$

$$k = 1,2,3,4,5$$

$$l^{th}\ observation = 135$$

$$\alpha = Machine\ Type\ \{CMM, FAROTIP, FAROLP\}$$

$$\beta = Degree\ \{0°, 5°, 10°\}$$

$$\gamma = Part\ \{1,2,3,4,5\}$$

Our model looks to compare machine, degree, and part, to test their impact on flatness. Because we are expecting to see differences between machine and degree, we have added the interaction effect between these two factors.

In order to apply ANOVA, a test for normality was performed. The measured data was distributed as shown in Figure 15. It can be seen that the data is skewed and does not follow a bell shape distribution. A Shapiro Wilk test proved that the data was not normally distributed.

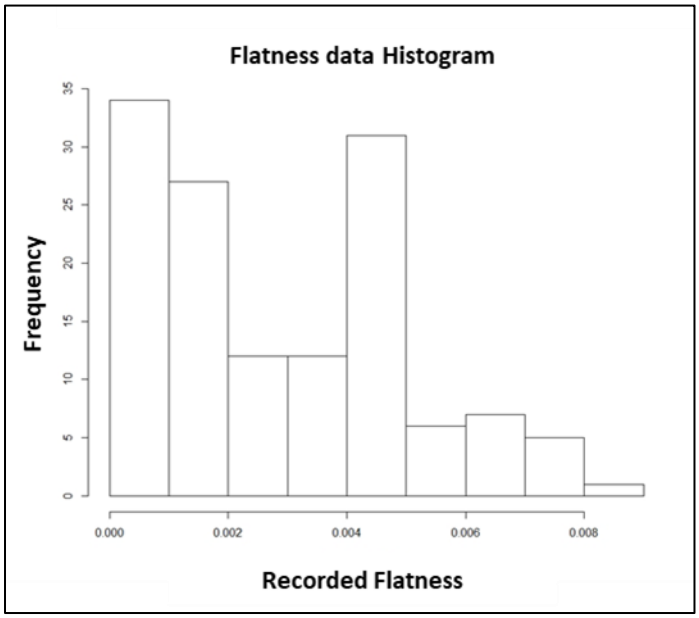

Figure 15. Recorded flatness data distribution

Therefore, we decided to transform the data by averaging the measured part flatness by machine and degree. This allowed us to have a single flatness value for each machine, degree, and part combination. The new table was used to conduct the ANOVA and check for the distribution of the residuals, which showed that the data was normally distributed, as presented in Figure 16. The Shapiro Wilk test of this data returned a $p - value = 0.95$, therefore proving that the transformed data (in this case, the experimental error) is normally distributed. Hence, as established by the assumptions of ANOVA, we were able to utilize the model to conduct the test.

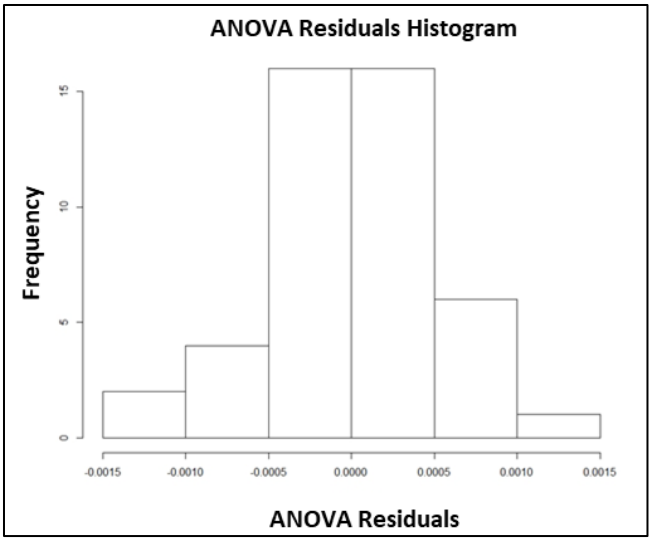

Figure 16. Residuals of ANOVA for transformed data distribution

The residuals plot shown in Figure 17, presents a satisfactory representation of the fitted data, while the Q-Q Plot in Figure 18 shows the shape of the distribution for the transformed data set.

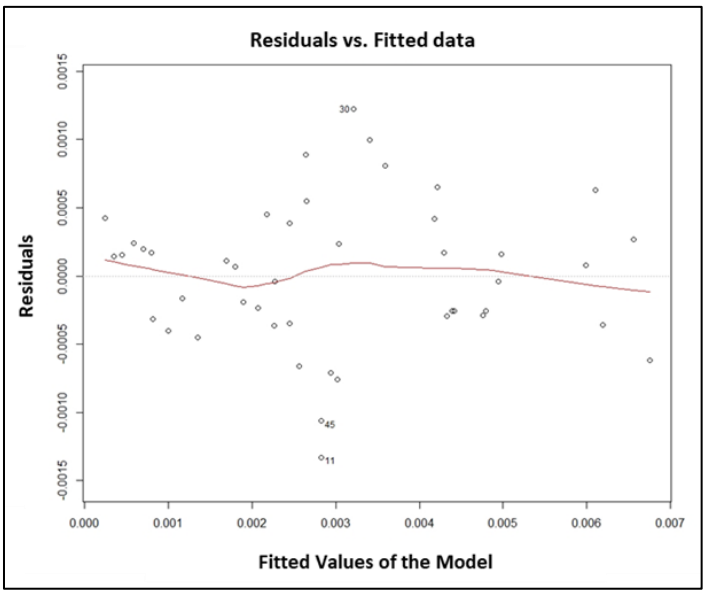

Figure 17. Residuals plot after the ANOVA with the transformed data

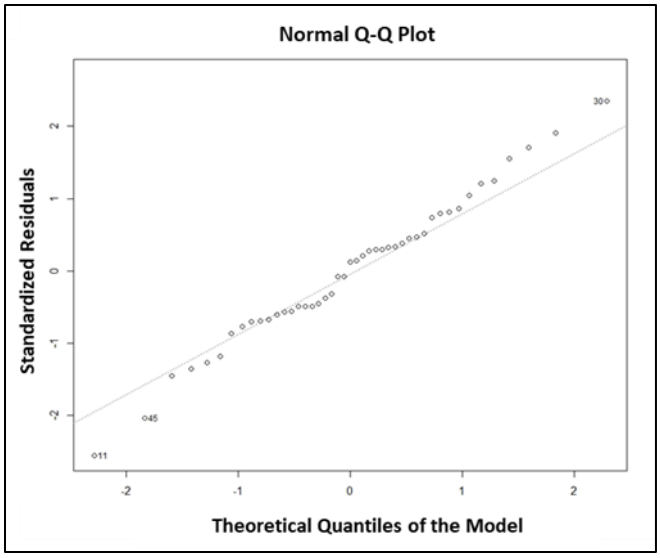

Figure 18. Q-Q plot of the residuals for ANOVA after transforming the data

When applying the model to ANOVA, the result is that machine, degree, and their interaction, was significantly different ($p - value < 0.05$). While part was not significantly different ($p - value > 0.05$). To understand which elements of these factors are distinct, a Tukey test was completed. It was found that for the machines, the CMM is significantly different to the AA-CMM contact and contactless method, while these two methods were significantly different from each other. In the case of the angle of the top face, 0° was significantly different to 5°, and this one was significantly different to 10°. However, there were not significant differences between 0° and 10°. When looking at the differences in the interaction effects more closely, we can see that there are two main patterns. When the CMM machine is being considered with 0° against the other machined parts, there are significant differences, and this makes sense as the flatness values recorded by the CMM on the non-machined (original cold drawn surface) part were considerably higher than those from the machined parts. Moreover, other significant differences can be observed when comparing the CMM machine and AA-CMM contact modality, against the AA-CMM contactless modality. The flatness values recorded by the laser, were substantially larger than the ones recorded by the other machines.

Now that we know all machines and some of the angles of a plane are statistically different when measuring flatness, we must determine what are the capabilities of each machine used. It can be seen on the data that all machines struggled when measuring the flatness of the 10° samples. The data points were more dispersed and the difference between the minimum and maximum values were higher than in any other combination of machine and degree. However, the Faro Laser Point performed the worst when looking at a part with that specific angle. That could be attributed to the way light from the laser might be reflecting from the material. Nevertheless, it is clear that across the different combinations, AA-CMM contactless method did not have as good of a resolution as the AA-CMM contact method and the CMM machine. The last two were close, but it is clear that for the measurements of 0°, 5°, and 10° cuts, the CMM was able to perform better than the AA-CMM contact method.

In order to create a boundary to the usability of these machines (capacity to obtain the flatness we are trying to measure), we could take three different approaches. If we would like to be conservative in the recommendations, we should select the maximum values presented in Table 6. Meaning for example, that if we had a flatness tolerance of $0.004\ in$ on a non-machined 0° cut aluminum surface, the CMM machine would be the only apparatus able to complete this task repeatedly, as all other options would not be capable of measuring that specific tolerance. For a more inclusive approach, the minimum values from Table 7 will become the limiters of the operational range of the machine. However, the inherent risk is that the machine might not perform reliably to measure tolerances to what is needed. Therefore, a balanced approach will be utilizing the averages as illustrated in Table 5. Averages will create boundaries where the machine has reliably obtained the data and allow the machines to be used in a wider range of tolerance levels, in turn making them more useful.

Lastly, for the gauge capability study calculations, we can see that when Precision-to-Tolerance is used, most machine-degree combinations are considered to have an adequate gauge capability. Except, when the contact method of the AA-CMM is being used for obtaining a tolerance of $0.0001in$. When looking at the other measures, the combination of CMM with 10° pieces, and AA-CMM contact with 10° pieces, have the highest percentage of observed contributed machine variance. This can be said, because when looking at the SNRs and DRs of calculated results of the aforementioned combinations, the results failed or were close to fail the given limits to evaluate adequate gauge capability. Meaning, that at those machine-degree combinations the gauge cannot be precise or accurate enough to be utilized in an inspection process regardless of its resolution.

CHAPTER 5: CONCLUSIONS AND RECOMMENDATIONS

5.1 Conclusion

This study sees the CMM perform better than the AA-CMM, because the CMM has a higher resolution; hence it is suggested to assign tasks to the machines based on the established capabilities discussed in this study.

CMMs and AA-CMMs have their own place in the manufacturing industry. Even though CMMs are better for metrology and feature verification, AA-CMMs such as the Faro Arm® are versatile and easy to use. It makes perfect sense for a shop to have either, or even better, both. Manufacturing environments are constantly evolving and working on different projects. So, depending on the working volume or tolerance level needed, these machines can be assigned to complete different tasks with the certainty that their performance will be appropriate for what is required.

To fulfill the goal of this pilot study, it is mentioned that a methodology and boundary must be created in order to provide the machinist or operators the opportunity to have a reference guide, such as the Machining Handbook for manufacturing operations. This one, however, will particularly guide workers and shops in selecting the appropriate tool for their metrology needs.

Capabilities can be defined in different ways. We have highlighted three: conservative, inclusive, and balanced approach. These are based on the results shown in Table 5,6,7. It is recommended to utilize a balanced approach to guarantee that the machines are being utilized to their potential, while making sure to not push them beyond limits that will make the machine unreliable.

Therefore, regarding the boundary of the machines for flatness verification, we utilized the values in Table 6, and determined that the CMM has a minimum measurable tolerance of

$0.002in$ for 0° non-machined surfaces, $0.0006in$ for machined 5° surfaces, and $0.0009in$ for machined parts with 10° surface cut. The AA-CMM contact has minimum measurable tolerance of $0.0032in$ for 0° non-machined surfaces, $0.0024in$ for machined parts with 5° surfaces cuts, and $0.0028in$ for 10° surfaces. Finally, the AA-CMM contactless has minimum measurable tolerance of $0.0045in$ for 0° non-machined surfaces, $0.0045in$ for 5° surfaces, and $0.0063in$ for 10° surfaces. In order to define the overall boundaries of the studied machines, we selected the minimum values of the average data in Table 6, which also happen to be all the values concerning the 5° cut parts. These overall boundaries can be seen as the minimum tolerance the studied machines can handle, which can be used to easily assigning tasks to the machines depending on the requirements of the project. The overall boundaries are as follows:

- CMM has a minimum measurable tolerance of 0.0006in
- AA-CMM contact, has a minimum measurable tolerance of 0.0024in
- AA-CMM contactless, has a minimum measurable tolerance of 0.0045in

It is clear from these observations and preliminary analysis that surface roughness and angles have an effect on the flatness data collected by the metrology devices studied. The gauge capability studies also showed that the machines were capable of measuring with precision certain combinations of machines and degrees, regardless of machine resolution. However, it can be concluded that some of the variance attributed to the machines, does not only relate to the machine itself, but to its operator.

Based on those boundaries, the metrology device selection process is proposed in Figure 19. An expanded version of these concepts can contain different setups for the two types of devices studied, other metrology devices, and brands. A database like this one could be applicable in the determining machine shop capabilities for an integrative procurement system.

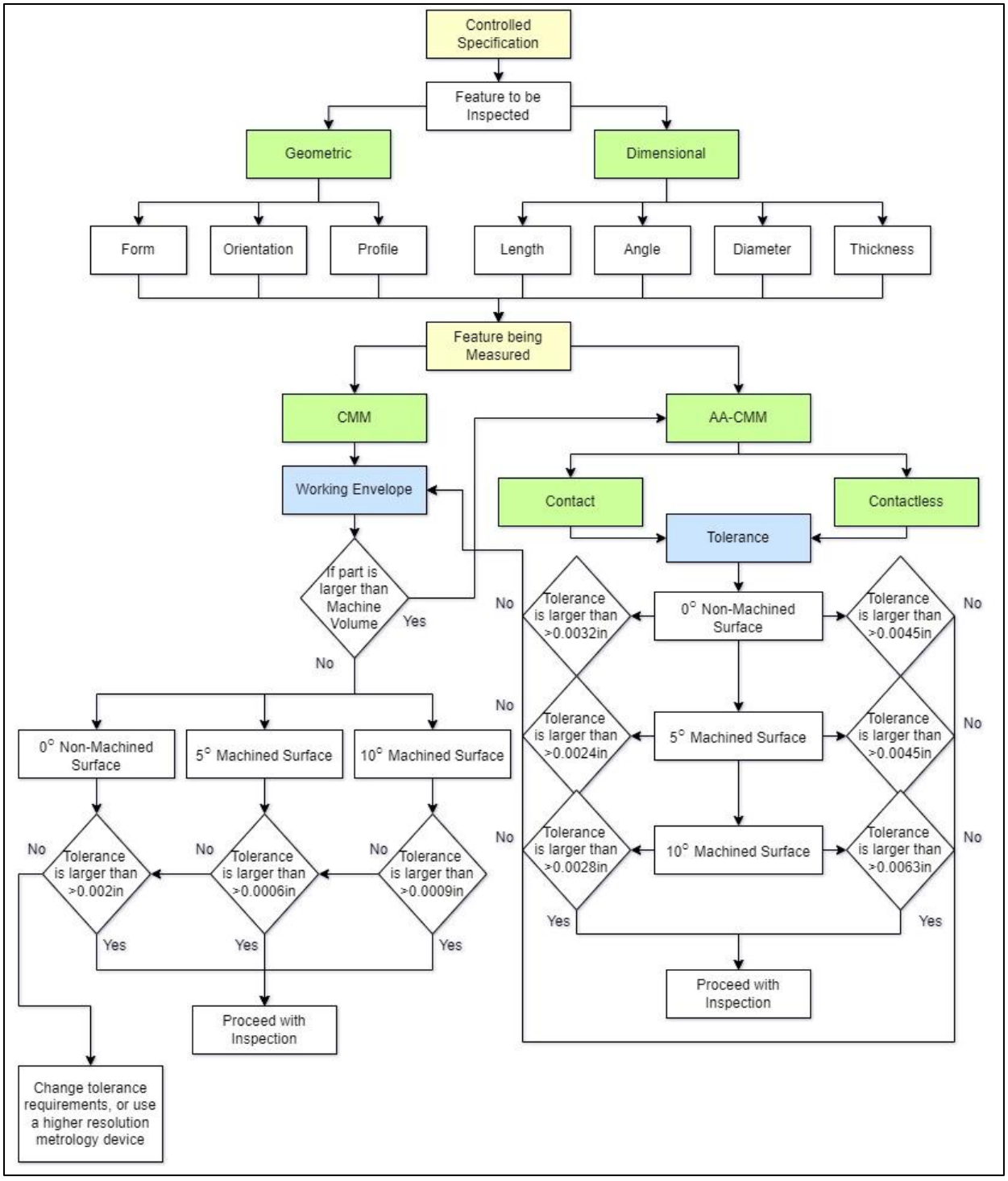

Figure 19. Flow diagram on the decision-making process for selecting a measurement device

5.2 Future Research

As mentioned in Chapter 2, the operator error is inherent when utilizing an AA-CMM. After experimenting, we can understand that an operator requires a certain level of experience and that, at the same time, taking measurement for prolonged periods of time can cause fatigue in the operator. Therefore, a similar experiment that accounts for user experience, or just multiple users, would be relevant, as we could quantify what part of the shortcomings in measuring with an AA-CMM comes from the operator or operator experience.

On this experiment 70 points were taken from a $2.5\ X\ 2.5in$ surface, which resulted on a point density of approximately 11 points per square inch. The effects of a part size increase should be studied, as it could become complicated having to collect twice as many points for a part twice as big. Understanding how many data points are needed based on surface size will directly impact the way in which we collect data, especially with AA-CMMs. Understanding how the amount of surface data points collected affect the created Best Fit plane in order to analyze the required tolerances, is imperative as manufactured parts footprint keep increasing.

Moreover, this thesis only studied one geometric form verification, flatness. It will be especially important to explore other geometric characteristics, like circularity or cylindricity, to expand the knowledge base methodology proposed in Figure 19, including changes in probe size, materials, and other CMM or AA-CMM device models.

Finally, this experiment was conducted utilizing a machined aluminum piece with no previous control values. To truly understand how far we are from the intended true value, repeating this experiment with a gauge or “perfect part” which was professionally manufactured and controlled, could help to properly identify the true differences between the CMM and AA-CMM methodologies studied.

References

AAA Testers. (n.d.). *Faro Platinum 8FT FaroArm Portable CMM Measurement Inspection Arm*. Retrieved May 2022, from AAA Testers: https://www.aaatesters.com/faro-platinum-faroarm-cmm-inspection-arm-platinumfaroarm-faro-platinum.html

Acero, R., Santolaria, J., Bra, A., & Pueo, M. (2016). Virtual Distances Methodology as VerificationTechnique for AACMMs with a Capacitive SensorBased Indexed Metrology Platform. *Sensors*. Retrieved April 2022

Cuesta , E., Gonzalez-Madruga, D., Alvarez, B., & Barreiro, J. (2014). A new concept of feature-based gauge for coordinate measuring arm evaluation. *IOP Science, 25*. Retrieved April 2022, from https://iopscience.iop.org/article/10.1088/0957-0233/25/6/065004

Cuesta, E., Alvarez, B., Barreiro, J., & Gonzalez-Madruga, D. (2014). A new concept of feature-based gauge for coordinate measuring arm evaluation. *IOP Science*. Retrieved March 2022, from http://iopscience.iop.org/0957-0233/25/6/065004

FARO. (n.d.). *How to evaluate flatness in GD&T*. Retrieved March 2022, from https://www.faro.com/en/Resource-Library/Article/how-to-evaluate-flatness-in-gd-t#:~:text=In%20application%2C%20one%20way%20to,the%20amplitude%20of%20the%20needle.

FARO. (n.d.). *Technical Specification Sheet for the Platinum, Titanium, or Advantage.* Retrieved May 2022, from FARO Knowledge Base: https://knowledge.faro.com/Hardware/Legacy-Hardware/Legacy_USB_FaroArm-ScanArm/Technical_Specification_Sheet_for_the_Platinum-Titanium-Advantage

GD&T Basics - Engineer Essentials. (2016). GD&T Basics - Flatness. Retrieved March 2022, from https://www.youtube.com/watch?v=AySConthyEM

Groover, M. (2010). *Fundamentals of Modern Manufacturing Materials, Processes, and Systems* (4th ed.). John Wiley & Sons, Inc. Retrieved March 2022

Gupta, N. (2017). Factors Relevant to Parallelism Inspection. SHAREOK. Retrieved March 2022, from https://shareok.org/bitstream/handle/11244/50871/2017_Gupta_Nitya_Thesis.pdf?sequence=1&isAllowed=y

Han, S., Chunlong, Z., Jianyu, C., & Shenghuai, W. (2021). Research on Micro/Nano Surface Flatness Evaluation Method Based on Improved Particle Swarm Optimization Algorithm. *Frontiers in Bioengineering and Biotechnology*. Retrieved April 2022, from https://www.frontiersin.org/articles/10.3389/fbioe.2021.775455/full#F7

Kalpakjian, S., & Schmid, S. (2014). *Manufacturing Engineering and Technology* (Seventh ed.). Pearson. Retrieved March 2022

Kim, W., & Raman, S. (2000). On the selection of flatness measurement points in coordinate measuring machine inspection. *International Journal of Machine Tools and Manufacture, 40*(3), 427-443. Retrieved March 2022

Lopez, A. (2019). Comparison of Discrete Part Verification Using Coordinate Measuring Machine and Articulated Arm Coordinate Measuring Machine. SHAREOK. Retrieved March 2022, from https://shareok.org/bitstream/handle/11244/323263/2019_Lopez_Andrea_Thesis.pdf?sequence=7&isAllowed=y

Lu, J., Gao, G., & Yang, H. (2013). Error Modeling and Analysis of Articulated Arm Coordinate Measuring Machines. *Advanced Materials Research*, 464-467. Retrieved April 2022

Metrology Deals. (n.d.). *B&S MicroVal PFx 454 CMM*. Retrieved from Metrology Deals: https://www.metrologydeals.com/product/bs-microval-pfx-454-cmm/

Montgomery, D. (2013). *Introduction to Statistical Quality Control* (7th ed.). John Wiley & Sons, Inc. Retrieved April 2022

Stephenson, D., & Agapiou, J. (1997). *Metal Cutting Theory and Practice.* Marcel Dekker, Inc. Retrieved March 2022

Trent, E., & Wright, P. (2000). *Metal Cutting* (4th ed.). Butterworth Heinemann. Retrieved March 2022

Vijayarangan, J. (2017). Non-Contact Method to Assess the Surface Roughness of Metal Castings by 3D Laser Scanning. Retrieved March 2022, from https://www.imse.iastate.edu/files/2018/01/VijayaranganJaipravin-thesis.pdf

Appendix

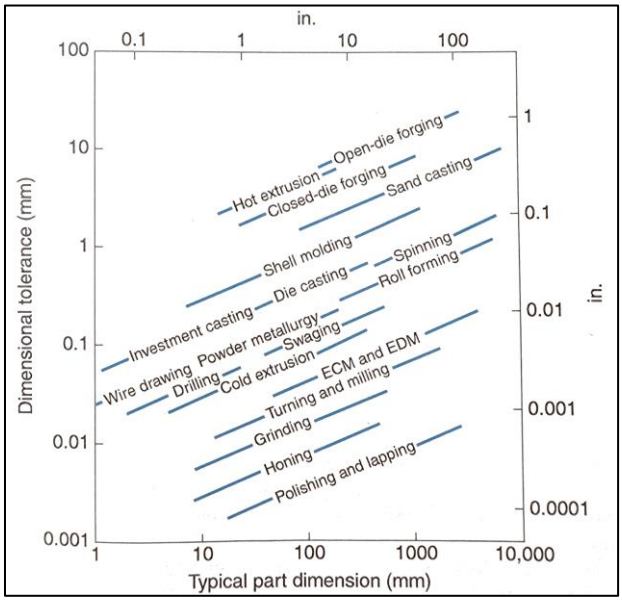

Figure 1. Dimensional tolerances as a function of part size for various manufacturing processes by Kalpakjian, et al.

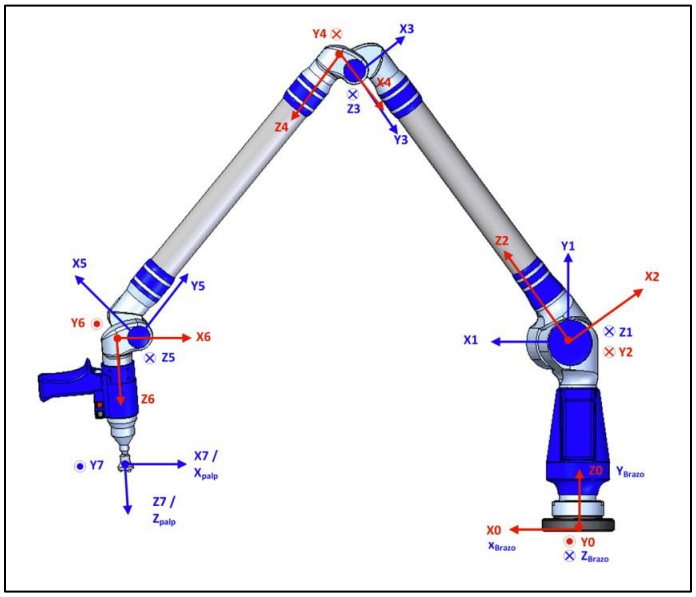

Figure 2. Faro Platinum coordinate reference system in the initial position according to D-H model by Acero, et al.

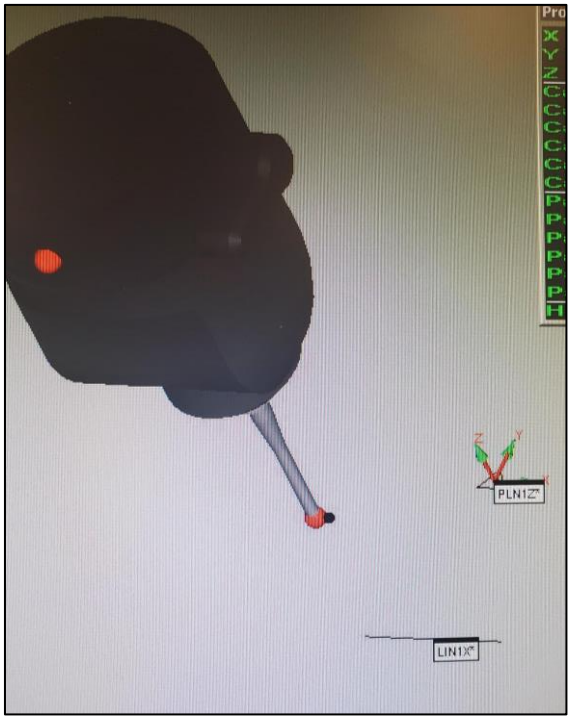

Figure A. Point for Y alignment marked by the CMM probe as shown by the software

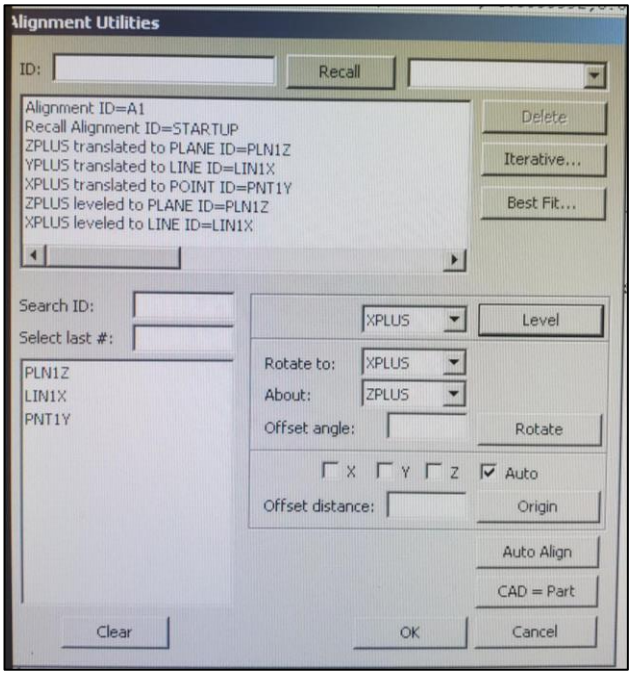

Figure B. Alignment settings to find the origin point where proposed in Chapter 3

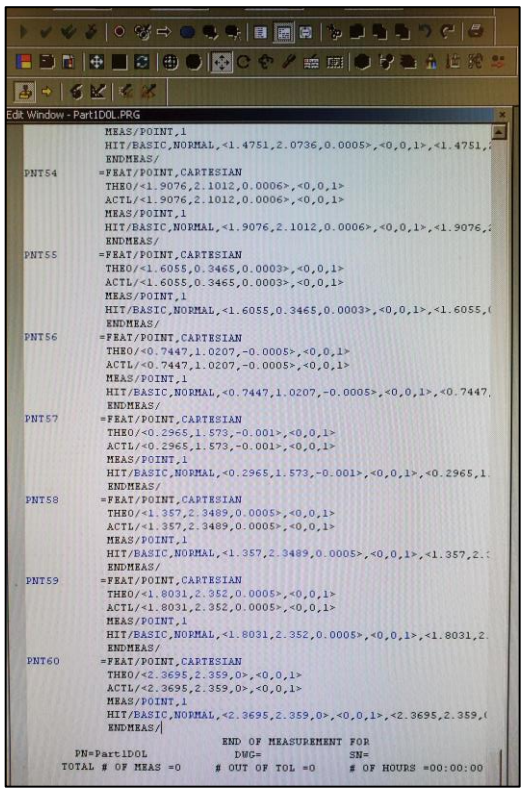

Figure C. Random points being collected on PC-DMIS to create the plane for Flatness analysis

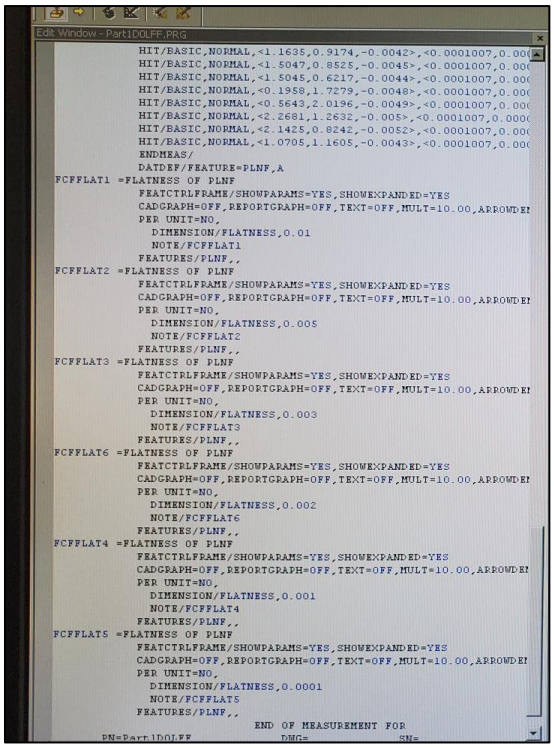

Figure D. Flatness codes created by the analysis program within PC-DMIS

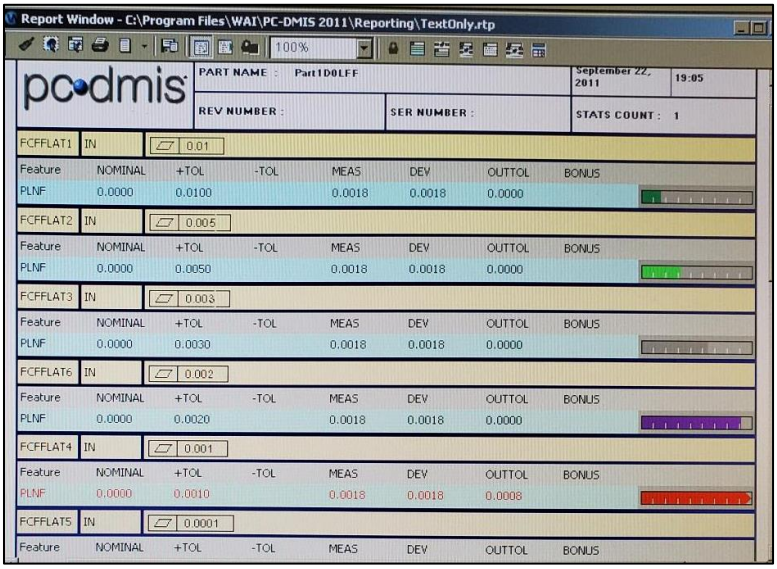

Figure E. PC-DMIS results for Flatness at different tolerance levels

RSTUDIO CODE FOR ANOVA

```
# Set Working Directory
setwd("")

# Import Data
data = read.csv("FINAL_Data_FINAL.csv")
head(data)

# Fixed
fixed_data = data[1:135, 1:4] # x, y

fixed_data$Machine <- as.factor(fixed_data$Machine)
fixed_data$Degree <- as.factor(fixed_data$Degree)
fixed_data$Part <- as.factor(fixed_data$Part)

# Using mean flatness

# Mean
 my_data= aggregate(fixed_data$Flatness, list(fixed_data$Part, fixed_data$Machine, fixed_data$Degree),
mean)
colnames(my_data) = list("Part", "Machine", "Degree", "Flatness")

# Setting the Factors
my_data$Machine <- factor(my_data$Machine)
my_data$Part <- factor(my_data$Part)
my_data$Degree <- factor(my_data$Degree)

# ANOVA
```

```
res.aov2 <- aov(Flatness ~ Machine + Degree + Part + Machine:Degree, data = my_data)
summary(res.aov2)
shapiro.test(res_aov2$residuals)

# Plot of Residuals
plot(res.aov2)
hist(res_aov2$residuals)

# Tukey Test
TukeyHSD(res.aov2, conf.level=.95)
```

RSTUDIO ANOVA RESULTS

```
               Df    Sum Sq   Mean Sq F value   Pr(>F)
Machine         2 1.187e-04 5.935e-05 154.805  < 2e-16 ***
Degree          2 6.160e-06 3.080e-06   8.027 0.001495 **
Part            4 3.750e-06 9.400e-07   2.445 0.066577 .
Machine:Degree  4 1.168e-05 2.920e-06   7.614 0.000199 ***
Residuals      32 1.227e-05 3.800e-07
---
Signif. codes:  0 ‘***’ 0.001 ‘**’ 0.01 ‘*’ 0.05 ‘.’ 0.1 ‘ ’ 1


        Shapiro-Wilk normality test

data:  res_aov2$residuals
W = 0.98944, p-value = 0.9515


  Tukey multiple comparisons of means
    95% family-wise confidence level

Fit: aov(formula = Flatness ~ Machine + Degree + Part + Machine:Degree, data
= my_data)

$Machine
                       diff          lwr          upr p adj
FAROLP-CMM      0.003955556  0.003399939  0.004511172 0e+00
FAROTIP-CMM     0.001608889  0.001053273  0.002164505 1e-07
FAROTIP-FAROLP -0.002346667 -0.002902283 -0.001791051 0e+00

$Degree
                 diff           lwr           upr     p adj
D10-D0  0.0001088889 -0.0004467272  0.0006645050 0.8804723
D5-D0  -0.0007244444 -0.0012800605 -0.0001688283 0.0083775
D5-D10 -0.0008333333 -0.0013889494 -0.0002777172 0.0023565

$Part
              diff           lwr          upr     p adj
P2-P1 1.111111e-04 -7.322921e-04 0.0009545143 0.9953133
P3-P1 2.037037e-04 -6.396995e-04 0.0010471069 0.9554726
P4-P1 5.740741e-04 -2.693291e-04 0.0014174773 0.3047497
P5-P1 7.592593e-04 -8.414393e-05 0.0016026624 0.0940492
P3-P2 9.259259e-05 -7.508106e-04 0.0009359958 0.9976874
P4-P2 4.629630e-04 -3.804402e-04 0.0013063662 0.5167419
P5-P2 6.481481e-04 -1.952550e-04 0.0014915513 0.1981881
P4-P3 3.703704e-04 -4.730328e-04 0.0012137736 0.7116065
P5-P3 5.555556e-04 -2.878476e-04 0.0013989587 0.3362031
P5-P4 1.851852e-04 -6.582180e-04 0.0010285884 0.9682779
```

```
$`Machine:Degree`
                                diff           lwr           upr     p adj
FAROLP:D0-CMM:D0         2.493333e-03  1.192258e-03  3.794409e-03 0.0000123
FAROTIP:D0-CMM:D0        1.140000e-03 -1.610754e-04  2.441075e-03 0.1237322
CMM:D10-CMM:D0          -1.100000e-03 -2.401075e-03  2.010754e-04 0.1521341
FAROLP:D10-CMM:D0        4.300000e-03  2.998925e-03  5.601075e-03 0.0000000
FAROTIP:D10-CMM:D0       7.600000e-04 -5.410754e-04  2.061075e-03 0.5924956
CMM:D5-CMM:D0           -1.446667e-03 -2.747742e-03 -1.455913e-04 0.0203000
FAROLP:D5-CMM:D0         2.526667e-03  1.225591e-03  3.827742e-03 0.0000097
FAROTIP:D5-CMM:D0        3.800000e-04 -9.210754e-04  1.681075e-03 0.9860575
FAROTIP:D0-FAROLP:D0    -1.353333e-03 -2.654409e-03 -5.225792e-05 0.0364618
CMM:D10-FAROLP:D0       -3.593333e-03 -4.894409e-03 -2.292258e-03 0.0000000
FAROLP:D10-FAROLP:D0     1.806667e-03  5.055913e-04  3.107742e-03 0.0017642
FAROTIP:D10-FAROLP:D0   -1.733333e-03 -3.034409e-03 -4.322579e-04 0.0029527
CMM:D5-FAROLP:D0        -3.940000e-03 -5.241075e-03 -2.638925e-03 0.0000000
FAROLP:D5-FAROLP:D0      3.333333e-05 -1.267742e-03  1.334409e-03 1.0000000
FAROTIP:D5-FAROLP:D0    -2.113333e-03 -3.414409e-03 -8.122579e-04 0.0001948
CMM:D10-FAROTIP:D0      -2.240000e-03 -3.541075e-03 -9.389246e-04 0.0000775
FAROLP:D10-FAROTIP:D0    3.160000e-03  1.858925e-03  4.461075e-03 0.0000001
FAROTIP:D10-FAROTIP:D0  -3.800000e-04 -1.681075e-03  9.210754e-04 0.9860575
CMM:D5-FAROTIP:D0       -2.586667e-03 -3.887742e-03 -1.285591e-03 0.0000063
FAROLP:D5-FAROTIP:D0     1.386667e-03  8.559125e-05  2.687742e-03 0.0296694
FAROTIP:D5-FAROTIP:D0   -7.600000e-04 -2.061075e-03  5.410754e-04 0.5924956
FAROLP:D10-CMM:D10       5.400000e-03  4.098925e-03  6.701075e-03 0.0000000
FAROTIP:D10-CMM:D10      1.860000e-03  5.589246e-04  3.161075e-03 0.0012086
CMM:D5-CMM:D10          -3.466667e-04 -1.647742e-03  9.544087e-04 0.9922767
FAROLP:D5-CMM:D10        3.626667e-03  2.325591e-03  4.927742e-03 0.0000000
FAROTIP:D5-CMM:D10       1.480000e-03  1.789246e-04  2.781075e-03 0.0163708
FAROTIP:D10-FAROLP:D10  -3.540000e-03 -4.841075e-03 -2.238925e-03 0.0000000
CMM:D5-FAROLP:D10       -5.746667e-03 -7.047742e-03 -4.445591e-03 0.0000000
FAROLP:D5-FAROLP:D10    -1.773333e-03 -3.074409e-03 -4.722579e-04 0.0022314
FAROTIP:D5-FAROLP:D10   -3.920000e-03 -5.221075e-03 -2.618925e-03 0.0000000
CMM:D5-FAROTIP:D10      -2.206667e-03 -3.507742e-03 -9.055913e-04 0.0000988
FAROLP:D5-FAROTIP:D10    1.766667e-03  4.655913e-04  3.067742e-03 0.0023383
FAROTIP:D5-FAROTIP:D10  -3.800000e-04 -1.681075e-03  9.210754e-04 0.9860575
FAROLP:D5-CMM:D5         3.973333e-03  2.672258e-03  5.274409e-03 0.0000000
FAROTIP:D5-CMM:D5        1.826667e-03  5.255913e-04  3.127742e-03 0.0015314
FAROTIP:D5-FAROLP:D5    -2.146667e-03 -3.447742e-03 -8.455913e-04 0.0001529
```